Fundamental modes of particle impaction on a solid object

Nils Erland L. Haugen* **and Steinar Kragset**
SINTEF Energy Research
7465 Trondheim, Norway
e–mail: nils.e.haugen@sintef.no

Anders Granskogen Bjørnstad
Department of Physics
The Norwegian University of Science and Technology

Summary In this work three fundamentally different modes of particle impaction on a cylinder in a cross flow is presented. Large particles impact on the cylinder in the so-called classical mode where the impaction efficiency is controlled by the particle inertia and the large scale fluid motions. For intermediately sized particles the thickness of the boundary layer around the cylinder is determining if a particle will impact on the cylinder surface or not. In this boundary stopping mode, the Reynolds number is important for the impaction efficiency. Finally, the smallest particles follow the flow perfectly around the cylinder, but due to their finite radius, some of them will nevertheless be intercepted. This is the boundary interception mode, and it is likely to be susceptible to secondary effects such as electrostatic forces, skin effects, surface roughness etc. Additionally, the effect of turbulence in the fluid flow is shown. It is found that for the relatively small Reynolds numbers investigated the effect of the turbulence is seen only in the boundary stopping mode.

Introduction

Particles impacting on the surface of an object in a cross flow are important for several different applications such as heat exchangers, filters and icing of airfoils.

For filters the aim is to trap as many particles as possible without too much pressure drop across the filter. This is the opposite goal of what one is after in a heat exchanger or on an airfoil where one wants to minimize the number of particles impacting on the object.

In industrial boilers the heat exchangers are typically tubes placed in the flue gas cross flow. In such a configuration it is crucial that particles embedded in the flue gas do not deposit on the tube as this will have detrimental effects on the efficiency of the heat exchanger both due to the reduced heat conductivity over the deposit layer and due to the increased pressure drop across the heat exchanger section. The deposit may also have drastic negative effects on corrosion. Two independent events must take place in order for a particle to deposit on a surface; first the particle must impact on the surface, and secondly it must stick to the same surface. Whether a particle sticks to the surface or not depends heavily on particle composition, surface composition and temperature. Typically ash particles from coal combustion are much less sticky than particles from bio mass combustion for a given temperature.

Numerical simulations

All simulations presented here are done with the Pencil-Code, which is a high order, massively parallel, open source direct numerical simulation (DNS) tool. The immersed boundary method has been utilized in order to incorporate the cylinder within the fluid flow. For more details see [1]. The governing equations for the fluid flow is written in the Eulerian framework, and are given by the momentum equation

$$\frac{\partial u_i}{\partial t} + u_j \frac{\partial u_i}{\partial x_j} + \frac{1}{\rho}\frac{\partial P}{\partial x_i} = \frac{1}{\rho}\frac{\tau_{ij}}{\partial x_j} \tag{1}$$

and the continuity equation

$$\frac{\partial \rho}{\partial t} + \frac{\partial}{\partial x_i}\left(\rho u_i\right) = 0 \tag{2}$$

when the stress tensor is

$$\tau_{ij} = 2\rho\nu\left[\frac{1}{2}\left(\frac{\partial u_i}{\partial x_j} + \frac{\partial u_j}{\partial x_i}\right) - \frac{1}{3}\frac{\partial u_i}{\partial x_i}\right], \tag{3}$$

u_i is the fluid velocity in direction i, ρ is fluid density, P is pressure and ν is the kinematic viscosity. In equations (1) and (2), summing over repeated indices is assumed.

The particles are treated within the Lagrangian framework and the evolution equations for particle position and velocity are given as

$$\frac{dx_i}{dt} = v_i \tag{4}$$

and

$$\frac{dv_i}{dt} = \frac{1}{\tau_p}\left(u_i - v_i\right), \tag{5}$$

respectively, when v_i and x_i are the particle velocity and position in the i'th direction. The Stokes time, which is the timescale for a particle to relax to the same velocity as the fluid flow, is given as

$$\tau_p = \frac{Sd^2}{18\nu(1+f_c)}. \tag{6}$$

Here is d the particle diameter, $S = \rho_p/\rho$ is the ratio between the particle density and the fluid density, and $f_c = 0.15\mathrm{Re}_p^{0.687}$ is a correction to the traditional Stokes law to account for Reynolds numbers larger than unity. The particle Reynolds number is $\mathrm{Re}_p = dv_{\mathrm{rel}}/\nu$ given that the relative velocity difference between the fluid and the particle is v_{rel}.

Results

By inserting Lagrangian particles in a fluid flow heading in the direction of a cylinder the impaction efficiency can be found as the ratio of the number of particles impacting on the cylinder to the number of particles which initially was moving towards the cylinder. In the following the particles will be characterized by the Stokes number, which is the ratio of the particle relaxation time and a typical timescale of the fluid. The Stokes number is the given as

$$\mathrm{St} = \frac{\tau_p}{\tau_f} \tag{7}$$

with $\tau_f = D/\overline{u}$, where D is the cylinder diameter and $\overline{u}$ is the mean flow velocity.

In Figure 1 a snapshot of the particle number density for $\mathrm{St} = 0.08$ (left), $\mathrm{St} = 0.3$ (middle) and $\mathrm{St} = 10$ (right) for a simulation with $\mathrm{Re} = 20$ are shown. Since this Reynolds number is sub-critical to the von Karman instability no unsteady eddies are seen behind the cylinder (black circle). For the lowest Stokes number essentially all particles are seen to follow the fluid flow around the cylinder, while as the Stokes number is increased to 10 a smaller fraction of the particles make it around the cylinder.

When increasing the Reynolds number to 400 it is seen in Figure 2 that von Karman eddies are now present as expected. Furthermore it is seen that for the lowest Stokes number particles

Figure 1: Snapshot of particle number per grid cell for simulation with Re $= 20$, and Stokes number of 0.08 (left), 0.3 (middle) and 10 (right). Grid resolution for this simulation was 1024x512 grid points. The relation between color coding and number of particles pr. grid cell is the following: 0 particles; white, 1 particle; black, 2 particles; blue, 3 particles; red, 4 particles; orange 5 or more particles; yellow.

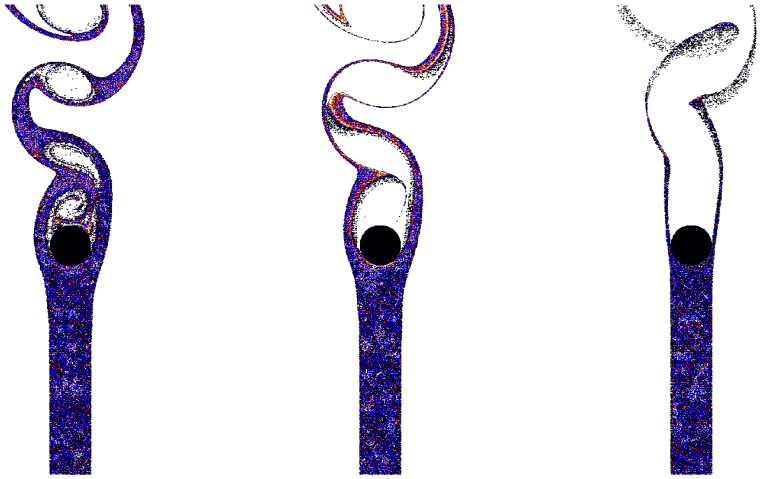

Figure 2: Snapshot of particle number density for simulation with Re $= 400$, and Stokes number of 0.08 (left), 0.3 (middle) and 10 (right). Grid resolution for this simulation was 1024x512 grid points.

are actually trapped in the small eddies on the back side of the cylinder, which make a few of these particles impact on the back side of the cylinder. For St $= 0.3$ the particles still do follow the flow reasonably well, but they are now too massive to be trapped on the back side of the cylinder. Finally it is seen that, as was also the case for the lower Reynolds number case, for the largest Stokes number most of the particles impact on the front side cylinder surface. It should be noted that for Re > 190 the flow is no longer purely two-dimensional as streamvise vorticity is generated [4], the flow is not yet turbulent for these low Reynolds numbers though. By running full three-dimensional simulations it has been verified that this three dimensionality

Figure 3: Snapshot of particle number density for simulation with Re $= 1600$, and Stokes number of 0.08 (left), 0.3 (middle) and 10 (right). Grid resolution for this simulation was 2048x1024 grid points.

has no measurable effect on the particle impaction efficiency.

For the Reynolds number of 1600 Figure 3 show that the particle behaviour is qualitatively similar to what is seen for Re $= 400$, with the exception that all structures in the eddies are much finer. This will also eventually lead to more particles depositing on the back side of the cylinder as a larger range of eddy sizes will be present on the back side of the cylinder such that several particle sizes might impact on the back side surface. For a Reynolds number of 1600 the flow will begin to break up into turbulence in the shear layers downstream of the cylinder [4], this is however not expected to have any effect on the particle impaction on the front side of the cylinder while it may have some effect on the particle impaction efficiency on the cylinder back side.

Non-turbulent inlet boundary conditions

The impaction efficiency is shown in Figure 4 where it is seen that for large Stokes numbers a large fraction of the particles will impact on the cylinder, while for Stokes numbers smaller than ~ 0.2 the impaction efficiency is very small. It is also seen that the the impaction efficiency clearly is dependent on the Reynolds number. This is particularly true for sub unity Stokes numbers.

Three different modes of impaction can be defined. For the largest Stokes numbers the classical impaction mode is found. When approximating the fluid flow with potential flow theory such that the entire flow field is described by stream functions the outcome is the classical mode of impaction [3]. For this mode the impaction efficiency is rather large, and almost independent of Reynolds number. This is due to the fact that for these large particles the boundary layer is not important, and the particle motions are controlled by the particle inertia and the large scale fluid flow. This is also why potential flow theory, which neglects viscous effects, gives an acceptable description of this mode.

In the boundary stopping mode the particles have less inertia, and they are being affected by

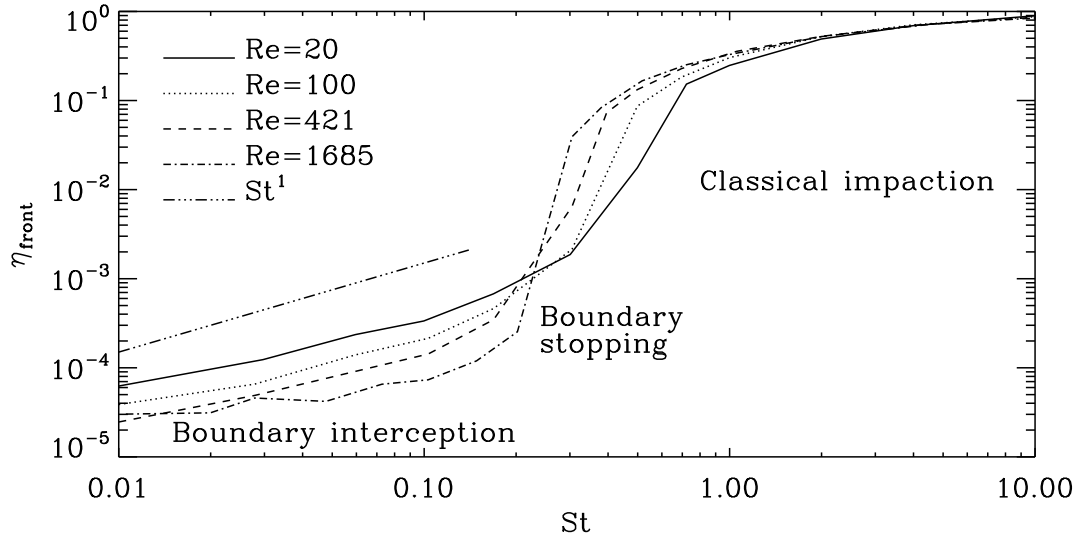

Figure 4: The three different modes of particle impaction for different Reynolds numbers.

the boundary layer around the cylinder. Since the Reynolds number define the boundary layer thickness this mode is strongly Reynolds number dependent. Furthermore the boundary stopping mode extends to larger Stokes numbers for smaller Reynolds numbers. In potential flow theory there is no boundary layer, and the boundary stopping mode is therefore not seen. Instead a minimum Stokes number for impaction is found below which no impaction occur. It is therefore clear that potential flow theory can not be used for sub unity Stokes numbers.

For Stokes numbers smaller than $\sim 0.1 - 0.2$ the third mode of impaction, the boundary interception mode, is found. Here the particles follow the fluid flow almost perfectly, but a few particles will still touch (impact on) the cylinder surface due to their finite radii. It has been shown in [1] that the the impaction efficiency should scale as the Stokes number for this mode of impaction. As is seen from the St^1 line in Figure 4 this is found to fit reasonably well with the data. It is expected that applying more subtle physical mechanisms such as van der Waals forces, skin effects, Brownian forces etc will have a significant effect on the impaction efficiencies of this mode.

Within the boundary stopping mode all impacting particles will impact within a rather small angle on the front side of the cylinder. The relevant timescale of the fluid flow is then no longer given by $\tau_f = D/u$, as used in the definition of the Stokes number, but rather by the inverse of the front side stagnation point velocity gradient;

$$\tau_{f,s} = \left(\frac{du_r}{dr} \right)^{-1} \tag{8}$$

when u_r is the radial velocity and r is the radius from the cylinder center. It is found in [1] that $\tau_{f,s} \approx \tau_{pot}(1 - B\mathrm{Re}^{-1/2})$ when τ_{pot} is the corresponding timescale based on potential flow theory and B is a constant. Lets now define a new non-dimensional number, instead of the Stokes number, where the fluid time scale is given by $\tau_{f,s}$;

$$\gamma_p = \frac{\tau_p}{\tau_{f,s}}. \tag{9}$$

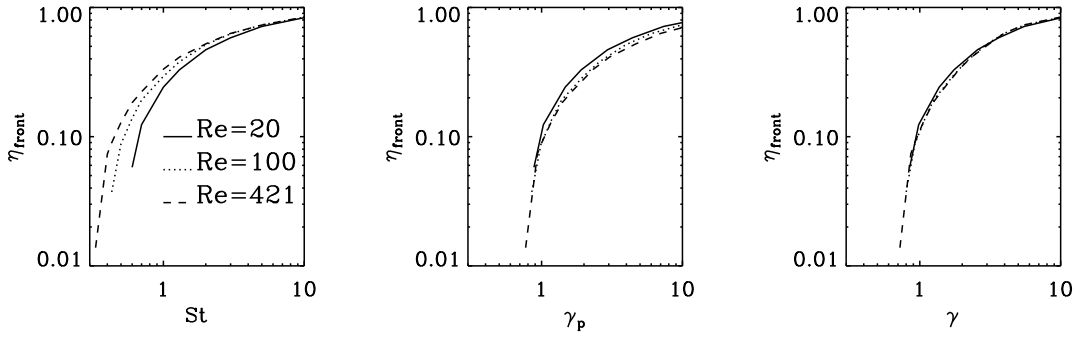

Figure 5: In the left hand plot the impaction efficiency is plotted as a function of the Stokes number, while in the middle plot it is plotted as a function of a new non-dimensional number based on the front side stagnation velocity gradient. In the right hand plot the impaction efficiency is plotted as a function of a smoothed function of St and γ_p. For all these data the effect of the boundary interception mode has been neglected.

It is shown in the middle plot of Figure 5 that the impaction efficiencies for the different Reynolds numbers collapse for small values of γ_p, unlike what they do when the impaction efficiency is plotted as a function of the classical Stokes numbers as seen in the left hand plot. For the data shown in Figure 5 the finite radii of the particles have been neglected. This effectively removes the boundary interception mode completely, because the particles with the lowest Stokes number now will follow the flow perfectly and cannot be intercepted by the cylinder. This is unphysical, but is done in order to more clearly see the effect of γ_p. For large Stokes numbers it is seen that plotting the impaction efficiency as a function of St instead of γ_p yields a better overlap of the curves for different Reynolds numbers. By defining a smooth interpolation between St and γ_p as

$$\gamma = \mathrm{St} f_s + (1 - f_s)\gamma_p, \tag{10}$$

when $f_s = \tanh(\mathrm{St}/5)$, three curves are found to collapse in the right hand side plot of Figure 5.

Turbulent inlet boundary conditions

In the previous section the inlet fluid flow was assumed to be laminar. This is however usually not a good assumption in most industrial applications. In this subsection isotropic turbulence at two different scales are inserted through the inlet. The turbulence is convected downstream towards the cylinder while decaying. In contrast to the non-turbulent simulations presented in the previous section the turbulent simulations are, due to the inherent three dimensionality of turbulence, done in three dimensions. In Figure 6 the impaction efficiency is shown as a function of Stokes numbers for two simulations with two different turbulent scales and compared with a laminar case. Two different turbulent scales have been simulated; one with an integral scale at a wavenumber of $k = 1.5$ and one with $k = 5$. The maximum turbulent fluctuation has been chosen to be around 80% of the mean flow velocity at the inlet of the simulation domain. The source of the turbulence is application dependent, but it could be e.g. channel flow generated turbulence, flame generated turbulence from a combustion chamber or some sort of mechanical turbulence generator. For channel flow generated turbulence the turbulence intensity would be smaller than 80%, while for the two other mechanisms mentioned the intensity is strongly application dependent. The value of 80% is chosen because it is fairly strong such that any possible effect should be clearly visible, but at the same time it is weak enough in order to avoid outflows

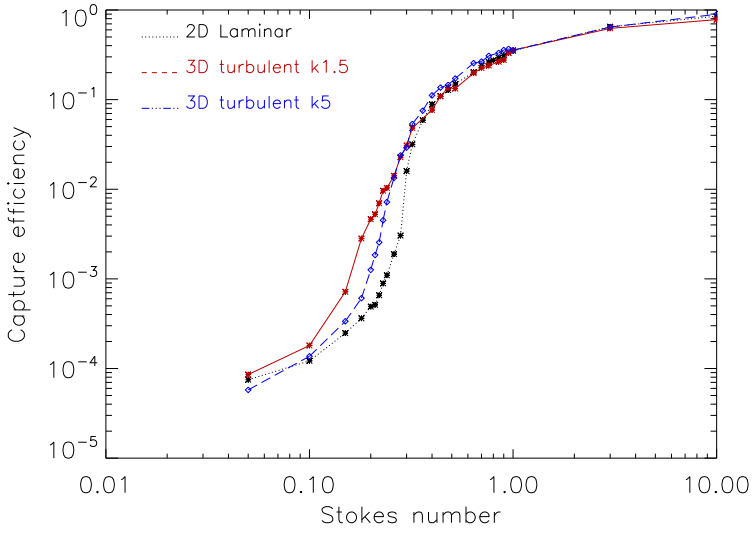

Figure 6: Impaction efficiency for two different turbulence scales compared with a laminar simulation. The Reynolds number is 400.

at the domain inlet.

It is seen that the turbulence has no effect for large Stokes numbers, but that the effect is significant in the boundary stopping mode.

The reason for this difference is the following: When a particle trapped in a turbulent eddy is approaching the cylinder, it will have a different velocity than the mean fluid velocity. Consequently, there will be a non-zero statistical variance σ^2 in the effective Stokes numbers of the intermediate and small particles. Considering St as a stochastic variable, the expectation $E[\eta(\mathrm{St})]$ of the impaction efficiency can then be approximated by

$$E[\eta(\mathrm{St})] \approx \eta(\mu) + \frac{\eta''(\mu)}{2}\sigma^2, \tag{11}$$

where $\mu = E(\mathrm{St})$. It can now readily be seen that if the second derivative of the impaction efficiency with respect to the Stokes number is positive, the impaction efficiency will increase with σ^2. In the boundary stopping mode, $\eta''(\mathrm{St})$ is indeed positive, whereas it vanishes in the boundary interception mode for the smallest particles. The larger particles in the classical mode are hardly affected by the turbulence, and thus the variance in the Stokes numbers is practically zero. As a result of this, the turbulence will alter the impaction efficiency only for moderate Stokes numbers, i.e. in the boundary stopping mode.

The above argument is confirmed by Figure 7, where the impaction efficiency is shown relative to the laminar case. The maximum relative difference is found to be almost a factor 10 for the large scale turbulence and a factor 6 for the small scale turbulence. The fluid Reynolds number for these simulations is 400 based on the mean flow velocity and the cylinder diameter. This number is rather small, which yields both a rather large turbulent energy decay and a rather thick boundary layer. Both these effects will have the effect of wiping out the effect of the turbulence. Furthermore the integral scale of even the turbulence with the smallest scale shown here are comparable to the diameter of the cylinder, and must therefore be considered large. In future work we will therefore consider larger fluid Reynolds numbers and also larger turbulent wavenumbers.

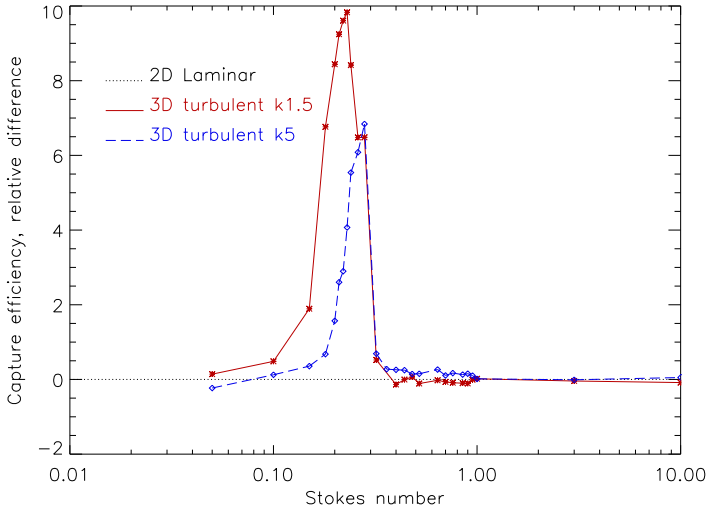

Figure 7: Impaction efficiency for turbulent simulations relative to laminar results. The Reynolds number is 400.

Conclusion

Three different modes of particle impaction on a cylinder in a cross flow has been found. For one of these modes can the impaction efficiency be considered to be almost independent of Reynolds numbers. The two other modes are very Reynolds number dependent. For industrial applications, such as heat exchangers, this can be utilized in order to reduce particle impaction. In fact, in [2] it was shown that changing the Reynolds number by only a factor of four might lead to a reduction in deposition of corrosive particles in a municipal solid waste incinerator by several orders of magnitude.

Finally the effect of turbulence embedded in the fluid flow has been investigated and found to have an effect in the boundary stopping mode, but except from this the impaction efficiency is almost independent on turbulence for the turbulent intensities and integral scales investigated.

Acknowledgements

This research project has been carried out within the framework of the EU FP6 project NextGen-BioWaste (019809) and within the Norwegian Research Council project PAFFrx (186933).

References

[1] N. E. L.Haugen and S.Kragset Particle impaction on a cylinder in a crossflow as function of stokes and reynolds number *Journal of Fluid Mechanics*, **vol.661**, 239, 2010.

[2] N. E. L.Haugen, S.Kragset, M.Bugge, R.Warnecke and M.Weghaus Particle impaction efficiency and size distribution in a mswi super heater tube bundle *Submitted for publication in Journal of the Institute of Energy*, 2011, http://arxiv.org/abs/1008.5040.

[3] R.Israel and D.Rosner Use of a generalized stokes number to determine the aerodynamical capture efficiency of non-stokesian particles from a compressible gas flow *Aerosol Science and Technology*, **vol.2**, 45–51, 1983.

[4] C. H. K.Williamson Vortex dynamics in the cylinder wake *Annual Review of Fluid Mechanics*, **vol.28**, 477–539, 1996.